Journal of NeuroEngineering and Rehabilitation

RESEARCH

Open Access

Post-traumatic hand rehabilitation using a powered metacarpal-phalangeal exoskeleton: a pilot study

Emanuele Peperoni[1,2*], Emilio Trigili[1,2], Eugenio Capotorti[1,2], Stefano Laszlo Capitani[1,2], Tommaso Fiumalbi[1,2], Foebe Pettinelli[3], Sara Grandi[3], Alberto Rapalli[3], Giulia Lentini[3], Ilaria Creatini[3], Nicola Vitiello[1,2], Elisa Taglione[3†] and Simona Crea[1,2*†]

Abstract

Background In the context of post-traumatic hand rehabilitation, stiffness of the hand joints limits the range of motion (ROM), grip strength, and the possibility of performing simple grasps. Robotic rehabilitation has been widely adopted for hand treatment with neurological patients, but its application in the orthopaedic scenario remains limited. In this paper, a pilot study targeting this population is presented, where the rehabilitation is performed using a powered finger exoskeleton, namely I-Phlex. The device aims to mobilize the metacarpal-phalangeal joint (MCP) in flexion-extension movements. The objective of the study was to verify the short-term efficacy, experience of use, and safety of I-Phlex in a clinical setting. As a secondary objective, the study verified the device's capability to measure clinically relevant variables.

Methods Six subjects with trauma-related illnesses of the right hand took part in the experiment. Passive and active range of motion (PROM and AROM) were recorded at the beginning and the end of the session by the therapist and by the exoskeleton. Experience of use was assessed through ad-hoc questionnaires and a numerical pain rate scale (NPRS). Safety was assessed by computing the number of adverse events during the operation.

Results Median increases in the PROM and AROM of 5.88% and 11.11% respectively were recorded among subjects. The questionnaires reported a median score of 93.83; IQR (85.01–100) and 80.00; IQR (79.79–93.75) respectively. No increase in the median NPRS was recorded among subjects between pre-and post-treatment. No major adverse event or injury to the patients was recorded. Only one malfunction was reported due to the brake of a transmission cable, but the patient reported no injury or discomfort. No statistical significance was observed between the ROM measurement recorded using the exoskeleton and the ones taken by the therapist using the goniometer.

†Elisa Taglione and Simona Crea senior authorship.

*Correspondence:
Emanuele Peperoni
emanuele.peperoni@santannapisa.it
Simona Crea
simona.crea@santannapisa.it

Full list of author information is available at the end of the article

Conclusions The device and related rehabilitation exercises can be successfully used in the clinical rehabilitation of the MCP joint. The device measurements are in line with the goniometer assessment from the therapist. Future studies will aim to reinforce the results obtained, introducing a control group to conclude on the specific contribution of the technology compared to conventional therapy.

Trial registration Hand Motor Rehabilitation Using a Wearable Robotic Device (WRL HX MCP), Clinicaltrials.gov ID NCT05155670, Registration date 13 December 2021, URL https://clinicaltrials.gov/ct2/show/NCT05155670.

Keywords Hand rehabilitation, Traumatic-hand patients, Exoskeleton, Self-alignment mechanism, Stiffness, Metacarpal-phalangeal joint, Robotic rehabilitation

Background

Hand injuries are among the main causes of hospitalization all over the world, accounting for up to 30% of the reported trauma cases [1–4]. The majority of hand impairments are caused by sharp injuries or blunt traumas, either procured at work or home environment [5]. They usually involve muscle-tendon structures and in some cases nerves, leading in many cases to complex medical conditions. When surgery interventions are necessary to restore hand or finger functions, post-surgery rehabilitation is paramount to reduce complications such as tendon adhesions at the level of the hand and fingers, which may ultimately affect the surgery results and the overall recovery [6]. Osteoarthritis is another major cause of loss of hand functionality and impairments, especially in the elderly population [7], leading to joint stiffness, reduced grip strength, and limited range of motion (ROM), therefore hampering the capability of the subjects to perform simple movements of daily life activities [8]. In general, hand limitations are highly disabling conditions that may induce depressive states [9], which can lead to slower recovery processes and increase the overall cost for the healthcare system [10].

Either traumas or osteoarthritis can cause the stiffening of the metacarpophalangeal (MCP) joint, which has a significant impact on overall hand functionality. Typically, the shortening of the collateral ligament due to surgical repairs or tissue damage makes the joint stiffer in a more extended position, hence, the ROM and the flexion capability of the finger are limited [11]. To improve these conditions, surgical interventions include arthroplasty and tendon release [12], whereas non-surgical approaches rely on rehabilitation programs based on the intensive mobilization of the joint [13], either passive (i.e. the physical therapist moves the patient's joint, while the patient remains passive) or active (i.e. the patient actively mobilizes his/her hand and fingers) [14, 15]. Following a trauma, whether in post-surgical scenarios or when surgery is not necessary, early rehabilitation is key to preventing tendon adhesions and muscle atrophy. Nevertheless, hand tissues and bones are fragile, and mobilization should be carefully dosed to avoid damaging healing tissues [16].

In the context of rehabilitation, wearable robotics is gaining momentum as a tool for therapists and clinicians to provide intense, repetitive, and engaging rehabilitation, tailored to the patient's abilities and with the possibility of gathering quantitative data on the recovery of the patient [17–20]. More specifically different robotic platforms for hand rehabilitation have been developed [21–23], exploiting two main design architectures, namely soft and rigid exoskeletons. Soft exoskeletons, also called *exogloves*, rely on stretchable fabrics that are connected to the user's body at specific anchor points; when actuated, fabrics produce tensile forces parallel to the underlying muscle and tendons and, in turn, generate torque at the joint level [24–27]; such tensile forces compress the underlying musculoskeletal system to generate joint torque. This architecture has the inherent advantage that there is no need for self-alignment mechanisms to ensure that forces are exerted in the correct direction, hence the fabric parts worn by the user are usually lightweight and simple to manufacture. The main drawbacks are related to the difficulty of embedding sensory systems, as high tensile forces may induce migration of the fabrics and sensors on the user's hand, and the high compression forces on the user's musculoskeletal system, which become critical when dealing with fragile, post-traumatic hands [28]. Rigid exoskeletons, in turn, need more sophisticated alignment mechanisms to transfer the torque around the user's joint safely and efficiently [29], but can embed sensory apparatuses to estimate relevant kinetic and kinematic joint variables (such as angles and torques). Actuation units could be coaxial to the joints or they might utilize a remote center of rotation [30–33], the latter option offering the advantage of reduced encumbrance on the user's hand.

The majority of clinical studies have been conducted to evaluate the efficacy of robotic hand exoskeletons with patients with spinal cord injury (SCI) or stroke survivors [34–36], while a few works focused on traumatic and post-surgical scenarios [37, 38]; while such studies open new perspectives on the use of exoskeleton technologies in post-traumatic hand conditions, they also highlighted limitations of the state-of-the-art systems in providing clinically-relevant measurements during the treatment.

We developed a powered finger exoskeleton, namely I-Phlex, for the treatment of joint stiffness in patients with orthopaedic impairments [39]. The device can monitor the torque and angle at the MCP joint and support finger flexion-extension movements with *active-assistive* and *passive* mobilization paradigms. Key features are a self-alignment mechanism for the MCP joint, a remote center of motion configuration, a series elastic actuation (SEA) for precise and reliable torque control, and a set of customized cuffs to connect the device with hands of different anthropometric dimensions.

The main objective of the presented study was to verify the short-term efficacy, experience of use, and safety of the I-Phlex with patients with orthopaedic hand impairments. Subjects participated in a single rehabilitation session with the device. Efficacy was evaluated by comparing the ROM measured by the therapist, before and after the robotic treatment; the experience of use was evaluated using an ad-hoc questionnaire and subjective evaluation of the pain via the Numerical Pain Rate Scale (NPRS); the safety of the system was evaluated by recording the number of hardware or software failures occurring during the use of the device. As a secondary objective, the study aimed to verify the capability of the device to measure clinically relevant variables, namely the active and passive MCP ROM. Hence, the active and passive ROM was measured via the I-Phlex exoskeleton and compared to the measures taken by the therapist via a goniometer.

Methods

I-Phlex Exoskeleton

I-Phlex (Fig. 1(a)) is a powered finger exoskeleton for the mobilization of the MCP joint of the long fingers, designed specifically for the treatment of post-traumatic joint stiffness. Three main features make the device suitable for providing repetitive joint mobilization while simultaneously measuring quantitative biomechanical parameters to evaluate the rehabilitation outcome. These features include (i) the kinematic chain with a self-alignment mechanism and a remote center of rotation, (ii) the compliant actuation, and (iii) the set of physical human-robot interfaces that connect the kinematic structure to the user's finger and hand.

Kinematic chain

The kinematic chain has a remote center of motion, virtually located at the MCP joint of the long fingers of the hand, and a self-alignment mechanism composed of two revolute (R) and one prismatic (P) joint, arranged in an RPR configuration. The first R joint is composed of a series of hinges connected by gears [40], allowing it to cover the physiological ROM of the MCP joint with low encumbrance on the dorsal side of the finger [39]. The slider-hinge joint of the kinematic chain (i.e., -PR) realizes the self-alignment mechanism for the MCP articulation, to minimize shear forces on the finger during the flexion/extension movement. Notably, the exoskeleton hand and finger cuffs are fastened in a 'zero position', namely with the finger fully extended ($\theta = 0$, θ representing the finger flexion angle). When the finger flexes at an angle θ, the kinematic chain configuration is univocally defined to ensure human-robot alignment and can be described by the rotation angle of the first hinge (α) and by geometric parameters, measured in the 'zero position'. Geometric parameters are: a, the distance between the contact point between finger and cuff (G) and the MCP joint (O_{MCP}), b, the distance between the slider-hinge joint (P) and G, c, the vertical distance between the exoskeleton joint (O) and O_{MCP}, and d, the distance between O and P. Detailed information related to the model of the mechanism can be found in [39]. A schematic representation of the self-alignment mechanism is presented in Fig. 1(a).

A direct kinematic model (DKM) relates the angles and torque measured by the exoskeleton to the anatomical variables (namely, MCP angle and torque), using anthropometric measures of the user's hand. To have an accurate estimation of the user's measurements, a calibration procedure was set up. The DKM and an inverse kinetostatic model (IKsM) were implemented on the device control system, based on a user-specific look-up table (LUT) obtained through the calibration procedure. The LUT sorts the values of the estimated MCP angle and MCP torque and relates them with the measured kinematic chain angle (α) and the SEA-measured torque (τ_{meas}^{SEA}). The sorted values are obtained by linear interpolation to ensure a smooth transition between the different elements of the LUT. Details about the model and estimation performance are given in [39].

Actuation unit

The actuation unit consists of a SEA, which enables torque measurement and control and ensures an intrinsically compliant human-robot interaction. The exoskeleton is fixed on a static support frame, housing a box for the control board and power electronics. The electronic box hosts a control electronics unit (NI SbRIO9651 processor, National Instruments, Austin, Texas, US) featured with both a dual-core ARM controller and a Field-Programmable Gate Array (FPGA) processor, a BLDC motor connected to a planetary gearbox 111:1 reduction ratio. From the gearbox, the actuator's shaft is connected to a miniaturized spring, embedded in the frame of the robot over the hand dorsum. The spring is the core of the SEA technology and has a stiffness of 2.89 Nm/rad. Two absolute magnetic encoders with 18 and 12-bit resolution are used to measure the spring deformation. The torque

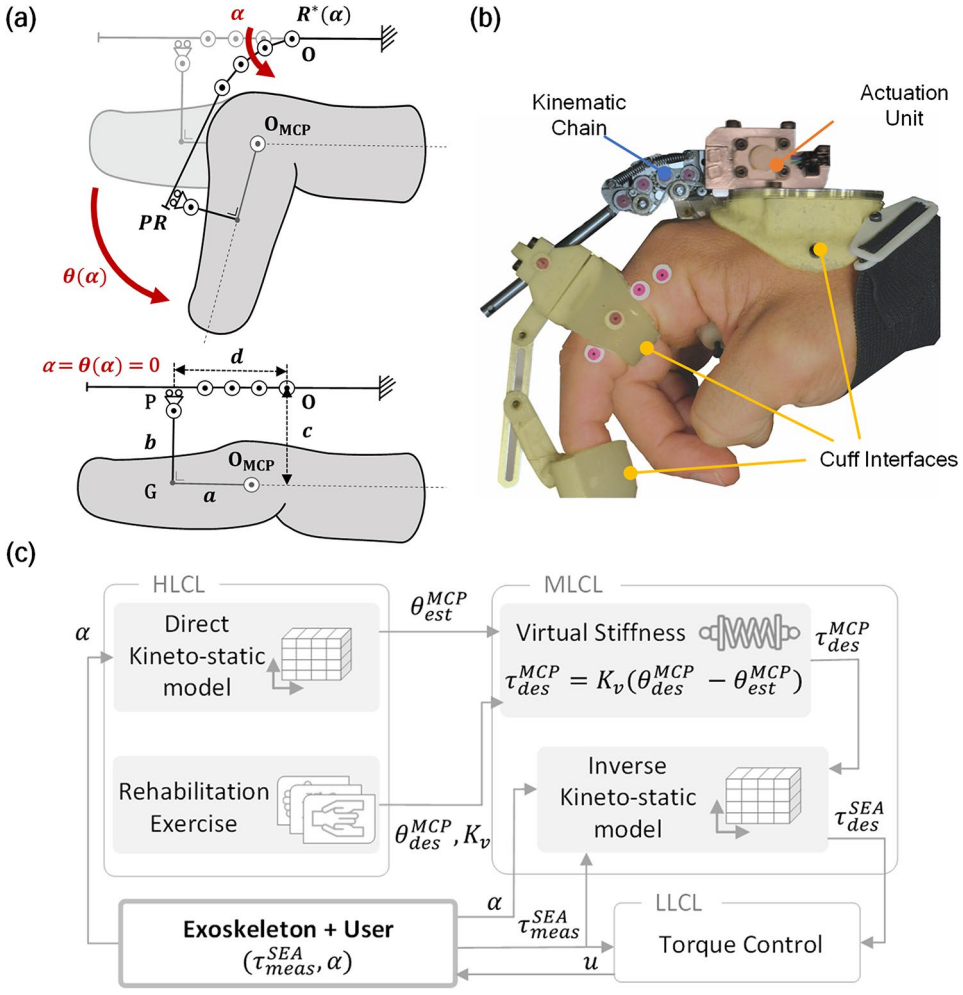

Fig. 1 (**a**) Schematic representation of the self-alignment kinematic chain of the I-Phlex exoskeleton. The mechanism is based on an RPR configuration, in which the first rotational joint is composed by a series of hinges. In the upper figure the rotational-prismatic-rotational joints are highlighted; in the lower figure, the self-alignment chain is depicted in the 'zero position' and the geometric parameters used the model are indicated. (**b**) Overview of the I-Phlex exoskeleton system worn by a user. The main components are highlighted. (**b**) Overview of the control algorithm for the platform operation. The HLCL is devoted to the estimation of the anatomical parameter of interest, i.e. the MCP angle θ_{est}^{MCP}. In the same layer, the user can select among different exercises through the exoskeleton GUI, which in turn determines the reference trajectory for the user θ_{des}^{MCP}. The rehabilitation paradigms are rendered in the MLCL by exploiting the impedance control strategy and modifying the controller gain according to the selected exercise modality (*passive* or *active-assistive*). Within the same layer, the reference torque trajectory (τ_{des}^{MCP}) for the LLCL is translated from the anatomical workspace to the robot once by exploiting an inverse kineto-static model (IKsM), implemented using patient-specific LUT. Finally, the LLCL is devoted to driving the actuation unit to apply the desired torque at the joint level, closing the loop on the measured torque from the SEA (τ_{meas}^{SEA})

resolution is 5 mNm and the maximum peak torque at the SEA is 1.5 Nm.

Physical human-robot interface (pHRI)

Concerning the physical human-robot interfaces, a library of hybrid rigid-soft interfaces has been designed to fit the device on different hand anthropometries. The exoskeleton interfaces with the hand dorsum and with the proximal and distal phalanxes via 3D-printed cuffs designed in different sizes. These cuff dimensions have been parametrized to speed up the scaling of the prototype based on the patient's finger dimension. The part in contact with the finger is realized in soft silicon-based material while the structural part is made of rigid biocompatible ABS plastic. The silicon components redistribute the pressure on the finger, which is critical in the case of traumatic hand patients which may present scars and sensitive skin areas. Moreover, this solution allows for an easy way to sanitize and clean the contact part of the device.

Control strategies and rehabilitation exercises

The I-Phlex control is based on a hierarchical structure [41], depicted in Fig. 1(c). The High-Level Control Layer (HLCL) and the Middle-Level Control Layer (MLCL) are implemented on the ARM real-time processor, running

at 100 Hz. The Low-Level Control Layer (LLCL) runs on the FPGA at 1 kHz.

The LLCL implements a *two-poles two-zeros* toque controller, which tracks the desired torque signal from the upper layer based on the error between desired and measured torque (τ_{des}^{SEA} and τ_{meas}^{SEA}, respectively). The output signal is sent to the exoskeleton driver, which sets the current input supplied to the motor. The controller performance ensures low residual stiffness when a null torque reference is required, (up to 0.17 Nm/rad at 1 Hz) while showing a root mean square error (RMSE) lower than 8mNm when following a desired reference torque profile, as reported in [39].

The MLCL runs an impedance control and the IKsM algorithms. The impedance control algorithm renders a virtual elastic behaviour of the device when following a reference trajectory; virtual spring stiffness can be tuned by the experimenter within a continuous range that spans between 0 and 10 mNm/deg, depending on the clinical scenario. In this work, two values of virtual spring stiffness were considered, to render relatively low virtual stiffness (namely, 5 mNm/deg) for an *active-assistive* rehabilitation paradigm, and relatively high virtual stiffness (10 mNm/deg) for rendering a *passive* rehabilitation paradigm. When null virtual stiffness is desired, the exoskeleton operates in the so-called *transparent* mode. Based on the desired MCP torque (τ_{des}^{MCP}) computed by the impedance control, the IKsM model computes the desired SEA torque (τ_{des}^{SEA}) via the user-specific LUT.

The HLCL allows the experimenter to select the type of rehabilitation exercise to run, estimate and visualize the variables of clinical interest (namely, the MCP joint angle, θ_{est}^{MCP}, and the MCP joint torque, τ_{est}^{MCP}), and implements a graphical user interface (GUI) for the patient that shows a reference angle trajectory and the θ_{est}^{MCP} in real-time. Based on the rehabilitation exercise, the user is required (or not) to actively try to follow the reference trajectory, while the device provides an assistive torque proportional to the reference and estimated angle error, using three possible values of virtual spring stiffness (null, 5 mNm/deg, 10 mNm/deg). In the different exercises implemented (Fig. 2), the reference angle trajectories were defined as minimum-jerk flexion/extension (F/E) cycles implemented with a fifth-order sigmoidal function, bounded within the patient's ROM measured at the beginning of the session. The duration of the sigmoid was computed to have a maximum speed of 10 °/s, hence, to avoid abrupt mobilizations that can injure post-traumatic hands, especially in post-surgery conditions. During the execution of the exercises, the GUI also displays indications of the progress of the exercise. Once the number of cycles (n_c) exceeds the predefined number or a certain time has elapsed, the session is concluded.

A predefined torque safety threshold, namely 0.45 Nm, is set for all the exercises to ensure that no harmful conditions for the patients occur. Moreover, a threshold over the allowable ROM is set so that the patient cannot exceed 5 deg above and below the maximum and minimum angles, respectively.

Experimental protocol

The experimental protocol was approved by the local Ethics Committee (Comitato Etico Area Vasta Nord-Ovest Toscana, protocol ID: HABILIS 2020; approval number: 18756) and the Italian Ministry of Health. Participants signed a written informed consent before

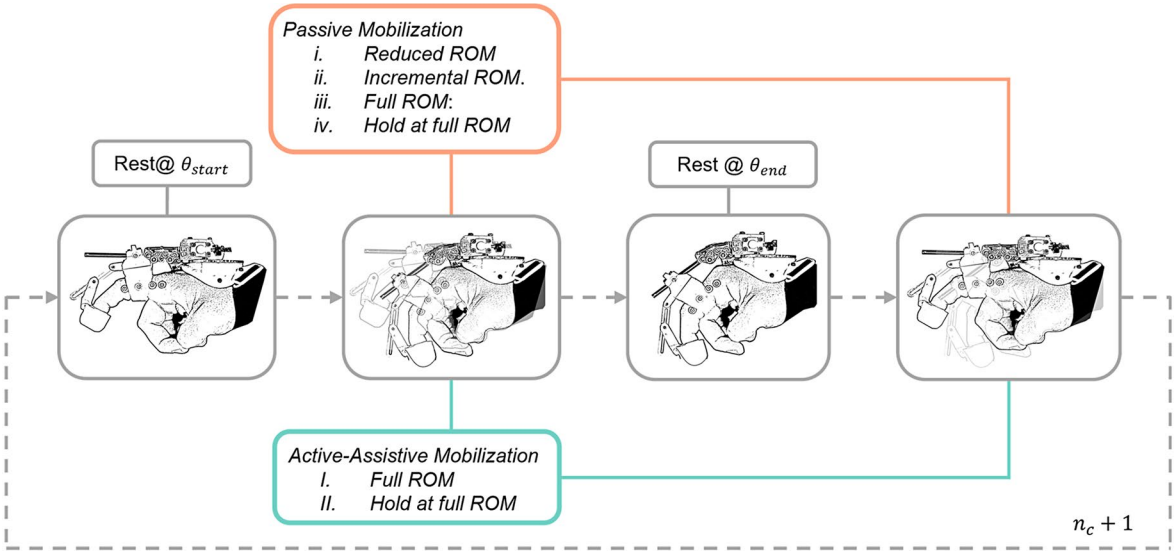

Fig. 2 Block diagram of the flexion-extension cycle for the different rehabilitation exercises. The exercises can be executed in *passive* or *active-assistive* modalities. Rest phases in flexed and extended positions have a duration that the experimenter can set. θ_{start} and θ_{end} refer to the starting and finishing position of the trajectory, according to the selected exercise to be performed

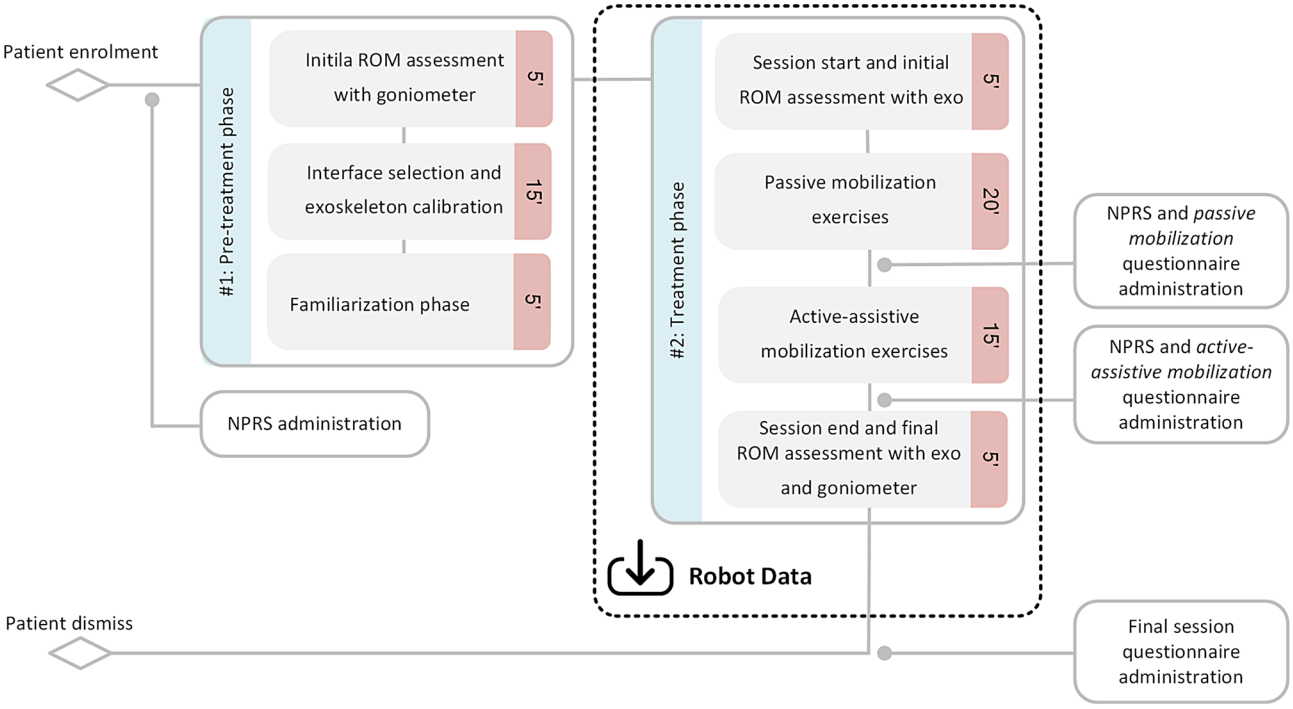

Fig. 3 Clinical protocol workflow. After enrollment, the patient proceeds to the pre-treatment and treatment phases. After each mobilization session, an ad-hoc questionnaire is administered to the patient. At the end of the treatment, a final session general questionnaire is administered and after the donning phase, the therapist assesses the patient's ROM. For each step of the protocol, an estimation of the duration is given in minutes

Table 1 NPRS administered questionnaire to evaluate the finger and hand pain during the exercises

0	1	2	3	4	5	6	7	8	9	10
(no pain)	(mild pain)			(moderate pain)			(severe pain)			

participation. The rehabilitation session with the I-Phlex platform lasted about 1 h. The session was structured in two distinct phases (Fig. 3). The pre-treatment phase was devoted to enrolment, evaluation of PROM and AROM by the therapist, system calibration, and familiarization of the patient with the device and exercises. Then, the treatment phase consisted of multiple trials of flexion-extension movements of the finger MCP based on various exercises.

Pre-treatment phase

a) *Initial MCP ROM assessment with a goniometer.* The MCP passive and active ROM (PROM, AROM) were assessed by the therapist through a goniometer.
b) *Administration of Numerical Pain Rate Scale (NPRS)*: NPRS was administered to assess the baseline condition before the treatment (Table 1).
c) *Selection of interfaces and calibration.* Anthropometric measurements of the anatomical sites of interest were measured and appropriate cuffs for the proximal and distal phalanxes were selected. The exoskeleton was worn and fastened to the patient's hand using straps. This phase lasted about 10 min. After wearing the device, the calibration phase required placing two markers on the patient's proximal phalanx ($\boldsymbol{F}1$ and $\boldsymbol{F}2$) and one as close as possible to the MCP centre of rotation (called *auxiliary* marker, $\boldsymbol{O_{aux}}$). These, in addition to the markers placed on the exoskeleton ($\boldsymbol{O}, \boldsymbol{A}, \boldsymbol{B}, \boldsymbol{C}, \boldsymbol{P}, \boldsymbol{G}$), compose the stereophotogrammetry system necessary for the calibration (Fig. 4). The therapist helped the patient to perform 10 F/E movements with the exoskeleton turned off. Then, from offline video analysis, markers' data were used to obtain the parameters for the LUT used in the middle-level control. The calibration procedure lasted about 5 min.
d) *Familiarization.* The exoskeleton was turned on and set in *transparent* mode to let the patient familiarize himself/herself with the device. If the subject manifested any discomfort or trouble with the device, the device was re-adjusted, and the calibration phase was repeated to ensure proper operation in the next steps.

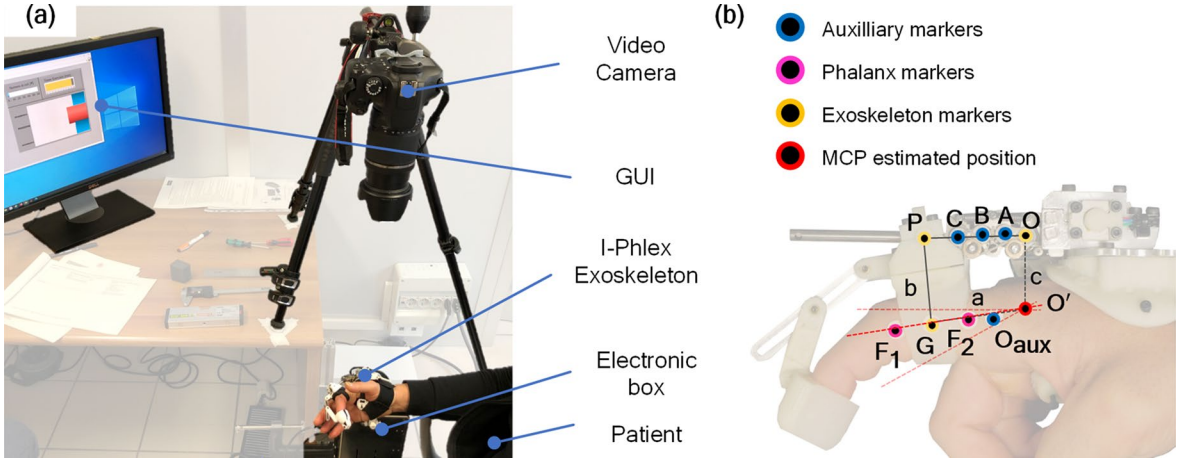

Fig. 4 (**a**) Setup for the clinical evaluation of the device. A video camera was used to acquire the data necessary for the calibration and to collect movement data during the therapy for offline processing. The patient wore the exoskeleton while sitting on a chair with the forearm held by the chair's arm. The reference profile for the joint angle (blue bars) was shown to the patient through a GUI displayed on a screen. (**b**) position of the marker on the finger and exoskeleton to perform the calibration procedure and LUT generation

Table 2 Questionnaire for the *passive* and *active-assistve* mobilization

Q1	The finger movement was perceived as natural during mobilization
Q2	The finger movement was perceived as smooth during mobilization
Q3	You were able to complete the exercises with ease
Q4	You were able to complete the exercises without experiencing muscle tension
Q5	You were able to complete the exercises without experiencing abnormal stress to the finger
Q6	You were able to complete the exercises without experiencing excessive stress to the finger

Treatment phase: the overall treatment was composed of four main phases

a) *Initial ROM assessment with exo*: at the beginning of the session, the patient, with the exoskeleton set in transparent mode, was asked to perform autonomously three F/E movements reaching the maximum flexion angle, and then to perform three F/E movements through the help of a therapist, similar to the procedure to measure the PROM. Data from the exoskeleton were acquired and used to compute the AROM and PROM of the MCP joint.
b) *Passive Mobilization.* In this session, the patient was asked to remain passive and let his/her finger move based on the action of the robot. The considered ROM for these exercises was the one measured from the exoskeleton during passive mobilization from the therapist (PROM). Four exercises were executed.

   i) *Reduced ROM*: the exoskeleton movement (reference angle trajectory) was set to span an angular range equal to 70% of the recorded PROM.
   ii) *Incremental ROM*: the angular range of the reference angle trajectory was initialized to 70% of the recorded PROM and the range was incremented by 5% of the PROM after each F/E cycle, up to 100% of the ROM. The procedure was repeated also decrementing the ROM.
   iii) *Full ROM*: the angular range of the reference trajectory corresponded to 100% of the recorded PROM.
   iv) *Hold at full ROM*: the exercise was executed at full PROM and each time the maximum flexion angle was reached, the exoskeleton kept the flexed position for a prolonged time (6 s).

After the exercises, the NPRS was administered together with ad-hoc usability questionnaires to evaluate the patient's experience of use with the device controlled in *passive* modality (Table 2).

c) *Active-assistive Mobilization.* In this session, the patient was asked to contribute to the motion by following a reference angle profile shown in the GUI (blue bars in Fig. 4). The considered ROM for these exercises was the one measured from the exoskeleton during active motion from the patients' movements inside the exoskeleton (AROM). Two exercises were executed.

   i) *Full ROM*: the reference angle was set to cover 100% of the recorded AROM.

Table 3 Final usability questionnaire for the evaluation of the device

Q1	It was easy to wear the device
Q2	It was quick to wear the device
Q3	The fastening system of the palm interface was comfortable
Q4	The fastening system of the finger interface was comfortable
Q5	You were satisfied with the safety of the device
Q6	You were satisfied with the functioning of the device
Q7	You felt comfortable while performing the exercises
Q8	You were able to perform the rehabilitation exercises
Q9	You would like to use the device in your rehabilitation program

ii) *Hold at full ROM*: the exercise was executed at full AROM and each time the maximum flexion angle was reached the patient was asked to keep the flexed position for a prolonged time (6 s) while the exoskeleton was switched to *transparent* mode.

After the conclusion of the exercises, the NPRS was administered again together with the ad-hoc usability questionnaires to evaluate the patient's experience of use with the device controlled in an *active-assistive* modality (Table 2).

d) *Pinch grasps.* After completion of the F/E exercises, the exoskeleton was set in *transparent* mode and the patient was asked to perform ten repetitions of pinch grasps by squeezing and relaxing a spongy object.
e) *Final ROM assessment with exo and goniometer.* At the end of the session, AROM and PROM were measured again through the exoskeleton. Then, the therapist and the experimenters helped the patient dress off the device. The therapist proceeded to measure the AROM and PROM with the goniometer. The duration of this step was about 10 min.

At the end of the treatment session, the patient was requested to reply to a questionnaire to evaluate the overall user experience with the device. The composition of the questionnaire is reported in Table 3.

Notably, after the completion of each session, the exoskeleton data were downloaded from the I-Phlex control unit and stored for offline analyses.

Study participants

Participants were recruited among people aged between 18 and 65 years with a traumatic hand injury. Patients in the postoperative phase after hand surgery were included in the study. Exclusion criteria included: (i) lack of cognitive capabilities to understand written consent form; (ii) use of electronic implantable devices (pacemakers or automated defibrillators); (iii) skin breakdown in areas in contact with the device's physical interfaces; (iv) occurrence of malignant neoplasms; (v) pregnancy; (vi) Numerical Pain Rate Scale higher than 6 in the pre-treatment phase.

A total of 6 participants (4 males and 2 females, age 56.16±6.40 years) were recruited within Centro di Riabilitazione Motoria Inail (Volterra, Italy) and provided written consent before the enrolment. Additional details about the subjects are reported in Table 4. ID06 was excluded from the analysis since during the therapy a transmission cable broke, and the experimental session was interrupted. Thus, the results are computed on five subjects who completed the treatment.

Outcome measures and data analysis

Different outcome measures were considered to assess the overall clinical efficacy of the treatment, experience of use, safety, and performance of the exoskeleton.

Clinical efficacy was evaluated by comparing the initial and final PROM and AROM values measured via a goniometer by the therapist. The experience of use was quantified by the outcomes of the usability questionnaires, administered after the treatment phases, and the NPSR evaluated before and after the treatment. The number of device-related adverse events was collected at the end of every session to evaluate the overall device safety.

Performance metrics were computed considering exoskeleton variables, namely the MCP angle estimation, θ_{est}^{MCP}, the estimated output MCP torque, τ_{est}^{MCP}, and the desired MCP torque τ_{des}^{MCP}. Moreover, the angle

Table 4 General data of the partecipants of the clinical study

	ID1	ID2	ID3	ID4	ID5	ID06
Age	59	49	49	55	65	60
Sex	M	F	M	F	M	M
Days After Injury	137	138	182	78	185	59
Type of Lesion	Multiple fracture at the upper limb	Amputation of index distal phalanx	Sub-amputation	Distal radius fracture	Fracture of wrist and hand	Fracture of the hand
Handedness	Right	Right	Right	Right	Right	Right
Previously Treated	No	No	No	No	No	No

measured by the camera, θ_{video}^{MCP}, was collected. Data were processed offline in MATLAB 2021 (MathWorks, Inc., Natick, MA, USA). The RMSE between θ_{est}^{MCP} and θ_{video}^{MCP} was computed to evaluate the performance of the exoskeleton in estimating the joint angle and compare it with the performance shown in a previous study conducted on healthy subjects [39]. The RMSE between τ_{est}^{MCP} and τ_{des}^{MCP} was also computed to quantify the capability of the device to track a desired torque profile in the final application scenario. Both indexes were assessed for the different exercises of the *passive* and *active-assistive* treatment sessions. Notably, in this study, only the flexion part of the F/E cycle was considered in data processing for the RMSE, as all the participants presented stiffness at the MCP joint that prevented flexion movement. Thus, the resistance to finger flexion was more informative about the status of the patient and functional to the final recovery. The SPARC index was computed on the θ_{est}^{MCP} variable to quantify the movement smoothness. The computation of the SPARC index in this study is the one proposed by [42]. The index was computed for each F/E cycle during the AROM measurement in the pre and post-treatment with the exoskeleton.

All indexes were computed for each participant and aggregated between subjects, and results are reported in terms of median (IQR) values. The SPARC index was compared between the pre-treatment and post-treatment conditions considering the median and IQR value of the metric.

The comparison between pre- and post-treatment PROM and AROM measured by the therapist was performed using the Wilcoxon signed-rank test (left tail) (the distribution of the data failed the normality test using the Shapiro-Wilk). In addition, the Wilcoxon signed-rank (two-tailed) test was used to compare the measurements collected with the goniometer by the therapist and those obtained by the device. Moreover, data obtained by the goniometer and the one measured by the exoskeleton were used to perform the Bald-Altman regression analysis and compute the Bias and Limits of Agreements (LoA).

Results

Figure 5 shows the ROM measurements obtained by the therapist in pre- and post-treatment assessments. Overall, the increase of the PROM and AROM were 5.88% and 11.11%, respectively. In both cases, the difference between pre- and post-treatment did not result in statistical significance but was close to the significance value ($p=0.06$, in both comparisons).

Figure 6 shows the results of the experience of use. The questionnaires administered on the *passive* and *active-assistive* mobilization reported a median score of 93.83; IQR (85.01–100) and 80.00; IQR (79.79–93.75) respectively (Fig. 6(a)). Patients gave higher scores in the *passive* mobilization, especially regarding the absence of muscle tension and stress. For two subjects, the naturalness and the smoothness of the movement were reduced during the exercises with the exoskeleton (Fig. 6(a)). The final questionnaire reported a median score of 84.73 with an IQR of (75.50–88.89) (Fig. 6(b)). The median of the NRPS was 1, 0, and 0, respectively in the *pre-treatment* phase, after the *passive* and after the *active-assistive* mobilization (Fig. 6(c)).

Four out of five participants wore the device finger-silicon interfaces with minimal discomfort. ID03, who wore

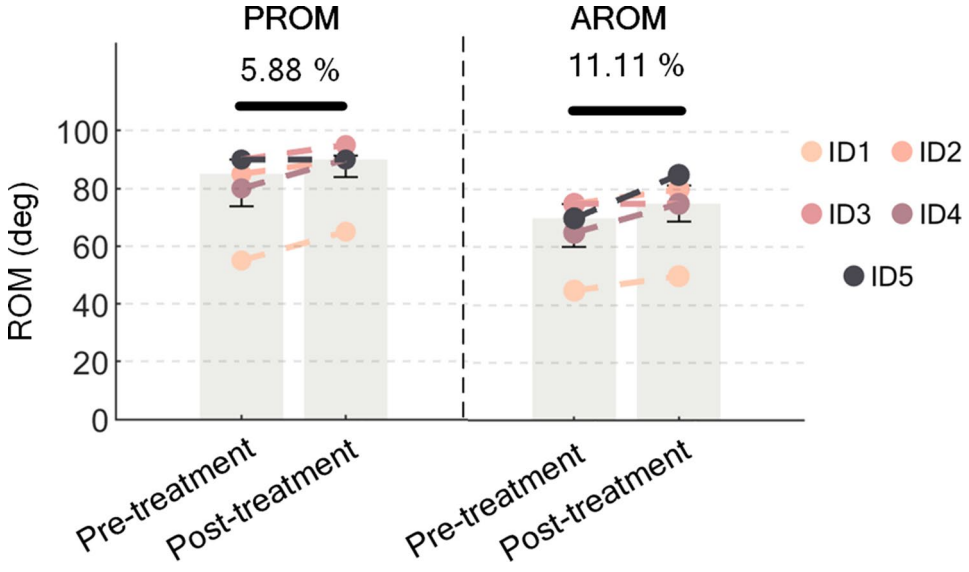

Fig. 5 Aggregated results for the PROM and AROM in the pre and post-treatment conditions and the indication of the median percentage of increment in the ROM. No statistical difference was reported ($p=0.06$ and $p=0.06$)

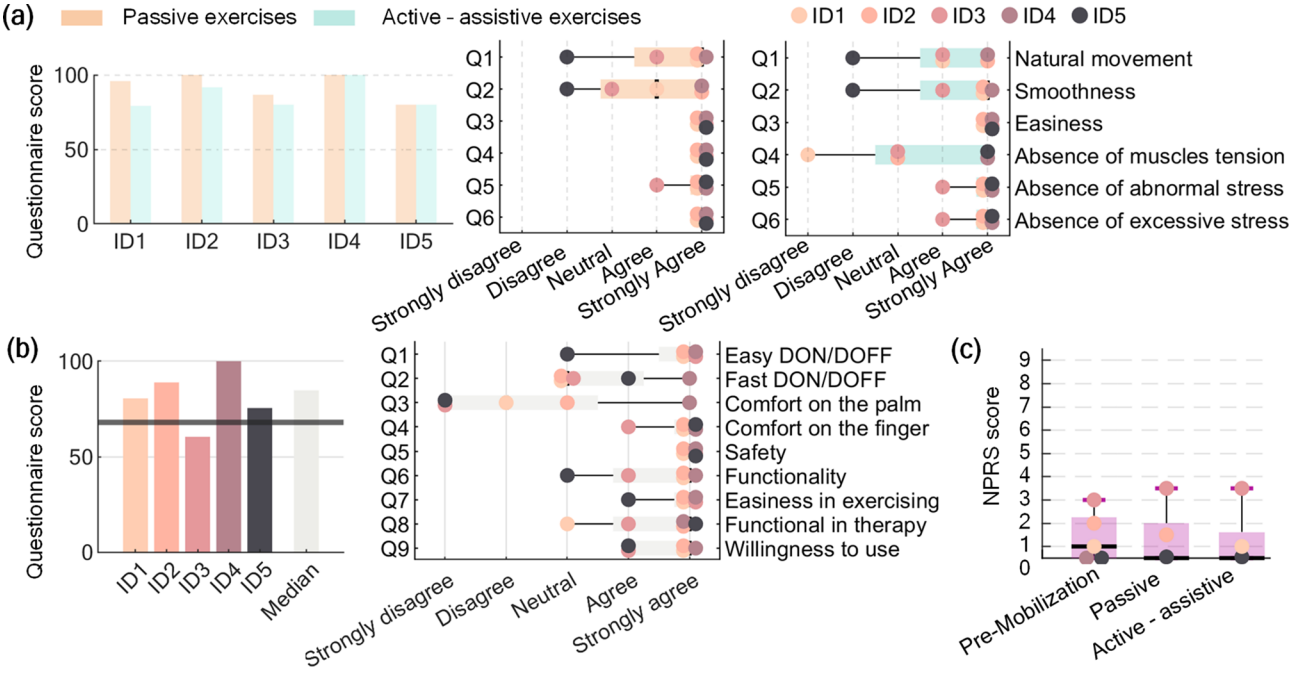

Fig. 6 Results on the user experience. (**a**) Results of the usability questionnaires for the *passive* and *active-assistive* exercises. (**b**) Results of the usability questionnaire of the device. The black line in the left graph highlights the threshold score for acceptance according to the SUS scale (68). (**c**) Results of the NPRS for the five patients

the exoskeleton with the palm interface not tightened due to scars on the palm side of the hand, gave the lowest score to the comfort of the interfaces. All participants could easily hold a correct sitting posture while wearing the exoskeleton during the rehabilitation sessions.

Regarding safety aspects, we reported one malfunctioning of the device, namely, the transmission cable broke during the test, and the experimental session was suspended. However, the malfunction had no consequences for the safety of the patient, as all the safety measures implemented in the device (hardware and software) functioned correctly. For the other 5 subjects, the prototype worked continuously for about 1 h in every session.

Performance indexes computed on the exoskeleton data are depicted in Fig. 7(a). For the *passive* mobilization, the RMSE of the estimated angle was 8.12 (5.87–9.04) deg, while the torque RMSE was 2.50 (2.05–2.60) mNm. For the *active-assistive* mobilization, the RMSE of the estimated angle was 6.86 (6.41–7.96) deg, while the torque RMSE was 1.80 (1.58–2.03) mNm.

Concerning the PROM and AROM measured with the exoskeleton, results show a median increment of the PROM by 15.94% and of the AROM by 9.60% (Fig. 7(b)). No statistically significant difference was observed between the measurement recorded using the exoskeleton and the one taken by the therapist using the goniometer within the same phase ($p=0.06$ for the pre-treatment, PROM; $p=0.31$ for the post-treatment, PROM; $p=0.63$ for the pre-treatment, AROM; $p=0.81$ for the post-treatment, AROM). Balt-Altman analysis resulted in a Bias of 4.70 deg and a LoA of (-22.91;32.31) deg (Fig. 7(c)).

Aggregated SPARC results from the subjects are reported in Fig. 7(d). Four out of five subjects improved the smoothness of the movement comparing the pre-treatment and post-treatment phases, with a median improvement of 0.7 points across the patients.

Discussion

Robot-mediated rehabilitation has been proposed to perform repeated mobilization of the impaired joints and limbs with control strategies that make the devices' behaviour adjustable based on the user's residual movement capabilities. Furthermore, the use of rehabilitation robots makes it possible to gather quantitative measures related to the patient's movement capabilities and monitor the rehabilitation progress, thus, in turn, adjusting the treatment [43]. Several hand rehabilitation robots have been proposed and experimentally verified in the state of the art [44–46]. Literature studies analysed the use of hand's wearable robots in neurological impaired conditions such as stroke, cerebral palsy, and SCI patients, reporting encouraging results in terms of increased clinical scale (DASH, Fugel-Meyer, and other) scores, improved dexterity after the training with exoskeleton in Box and Block test, and ultimately improved functional performance during the ADL [34, 47]. On the other hand, few studies focus on the treatment of trauma-related

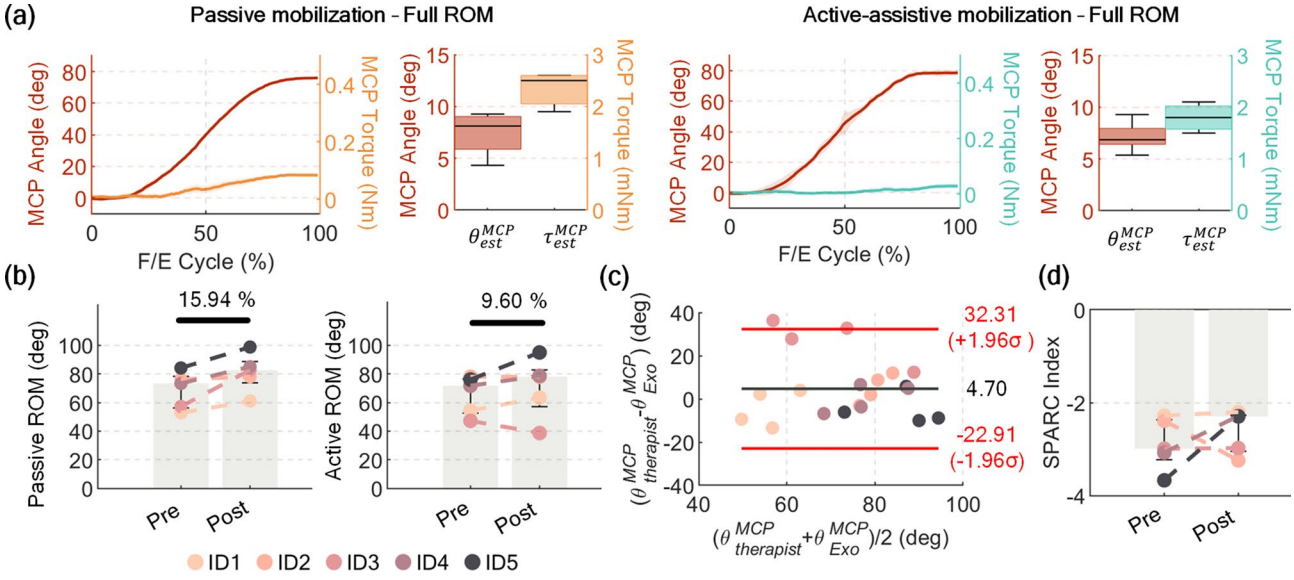

Fig. 7 Exoskeleton performance metrics results. (**a**) The mean MCP angle and torque profiles are reported for one representative subject in the *Full ROM* exercise in the *passive* (left) and *active-assistive* modality (right). The RMSE for θ^{MCP} and τ^{MCP} are reported, aggregated for all participants. (**b**) The PROM and AROM measured using the exoskeleton before and after the treatment are reported, together with the indication of the median percentage of increment in the ROM. (**c**) Result of the Bald-Altman analysis of the measurements taken by the therapist and those obtained using the exoskeleton (**d**) Aggregated results for the SPARC index evaluated pre- and post-treatment. In the figure, Pre and Post stay for pre-treatment and post-treatment conditions

hand stiffness with robotic-mediated rehabilitation [37, 48, 49].

The presented work introduces a wearable robotic platform for the rehabilitation of post-traumatic hands. The objective of this study was two-fold: (1) to verify the short-term efficacy, the experience of use, and the safety of the presented device within the framework of orthopaedic rehabilitation, and (2) to assess the capability of the device to measure clinically-relevant variables such as the active and passive ROM, the movement smoothness and the interaction torque at the joint. To achieve these preliminary objectives, the study consisted of a single rehabilitation session.

Efficacy was quantified by the PROM and AROM in pre- and post-treatment, measured by the therapists using a goniometer. Indeed, the ROM is commonly monitored in clinical practice to quantify the progress of the rehabilitation (within the session and across multiple sessions), as this measure is very easy, fast, and repeatable to perform [50, 51]. The single-session mobilization with the I-Phlex device resulted in a median percentage increase of 5.88% and 11.11%, respectively for the PROM and AROM. Despite not being statistically significant, the increase was very close to the significance value (i.e., 0.05), hence showing a trend toward significance. In absolute terms, the increase of the ROM showed a median value of 6 deg both for the AROM and for the PROM, which is close to the minimal clinical significance reported in the literature [52]. Overall, these results suggest that the therapy with the I-Phlex may induce an increase in the active and passive ROM of the MCP joint, thereby reducing joint stiffness. Notably, the results were achieved using a combination of *passive* and *active-assistive* exercise paradigms within a pre-defined sequence. Due to the preliminary nature of this study, the type, duration, and sequence of exercises were kept the same for all participants, and minimal customizations were made to the exercises (namely, the exercises were set according to the initial PROM and AROM measured at the beginning of the session). This configuration of the study allowed us to verify that the whole spectrum of exercises implemented on the platform can be applied to diverse types of clinical conditions; however, from the perspective of the clinical efficacy of the treatment, it is likely that different patients may have benefited more from different subsets of rehabilitation exercises and the improvements recorded in this study may be even larger with proper customization of the therapy. In similar literature studies, the overall increase in the finger flexion ROM stated around 8.3±20.2 deg as reported from [53]; in [54] the reported mean ROM in extension stated around 10 deg, while in [55] comparison of the total active ROM (i.e., the sum of the ROM at each finger joint) results to be statistically significant when comparing the treatment of post-traumatic hand subjects using robotic rehabilitation. Thus, the presented results are in line with the current state-of-the-art, but even higher increases could be achieved with patient-specific customization of the treatment.

The safety and stability of the platform were assessed by monitoring the platform's behaviour during the clinical study. Within the present clinical study, the system operated in total for about 10 h and, during each of the five rehabilitation sessions, for about one hour continuously. During the experimental trials, the patients were able to complete the exercises without any reported discomfort or abnormal pain deriving from the use of the device. One malfunction occurred, which was related to the brake of the transmission cable in the kinematic chain, which did not cause any pain or discomfort to the patient. For every subject recruited in the study, the pHRIs of the exoskeleton were able to fit the distinctive anthropometries, despite the differences in body size, sex, and level of impairment. Four out of five subjects wore the exoskeleton with minimal discomfort and effort, and after one hour of exercise, no major alteration of the skin surface was notified by the clinical staff. For the ID03, the exoskeleton was worn with the only burden that the hand interface was left loose since the subject presented scars on the palm that prevented a strong fixation.

Questionnaire scores were used to evaluate the users' experience with the device and its suitability for use in a larger-scale study. The result of the general questionnaire on usability showed a median score of 89.17, meaning that the platform was found to be usable in the clinical scenario for which it was designed (the threshold for usability was set to 68 points, as in [56]). The ad-hoc questionnaire for *passive* and *active-assistive* exercises showed that the devices allow for a smooth and natural movement both while operated in *passive* and *active-assistive* modalities, without excessive/abnormal stress and abnormal muscle tension. Finally, the results of the NPR scale did not increase after therapy for most of the subjects, meaning that the therapy was not perceived as harmful by subjects. Only one subject, ID3, reported an increase of 1 point with respect to the *pre-treatment* condition. Such increase may be related to the intense mobilization per se, and not specifically to the use of the device, due to the presence of scars on the palm that may be stretched during the rehabilitation.

Considering the comparison of the exoskeleton and therapist measurements of the PROM and AROM, no statistically significant difference was found between the sets of measurements, with significance values higher than 0.30 in three out of four comparisons, showing considerable alignment between the two measurement systems. Moreover, Bald-Altman analysis shows that most of the sample measurements resulted within the LoA, indicating an agreement between the goniometer measures and the exoskeleton ones. In some cases, the difference between the measurements spans over the LoA burdens, although, the reported measurements are coming from ID03, thus suggesting that the good fit of the interfaces is a mandatory step to collect trustable measurements using the exoskeleton.

Considering the accuracy of the exoskeleton measurements throughout the whole ROM, we compared the assessment of the angle by the platform to a video ground truth and the results showed that the error was about 7 deg. This result was in line with previous characterization carried out with healthy subjects in laboratory conditions [39]. This average error may, at least in part, explain the difference observed with the ROM measured using the goniometer. It is worth noticing that the I-Phlex measures were able to capture the relative differences between the pre- and post-treatment conditions [57, 58].

Concerning the accuracy of the low-level torque control, median RMSE torque resulted equal to 2.50 mNm for the *passive* exercises and 1.80 mNm for the *active-assistive* ones, indicating that the exoskeleton can track the desired torque profiles with appropriate performance (error was 1.5% of the peak desired torque). Across subjects, the maximum torque ranged between 0.07 Nm and 0.17 Nm for the *passive* exercises and between 0.04 Nm and 0.12 Nm in the *active-assistive* exercises. The reported values are in line with the biomechanical expected values reported in [59] and comparable to other devices presented in the state-of-the-art [53, 54].

SPARC index was evaluated for each subject before and after the treatment. The results demonstrate an overall decrease in the SPARC index when comparing the pre- and post-treatment conditions. Specifically, four out of five participants exhibited a reduction in the interval ranging from 0.01 to 1.38, while one participant displayed an increase in the index relative to the pre-treatment condition of -0.85. Therefore, these findings suggest a potential association with reduced activity during *active-assistive* exercise possibly due to participant fatigue or decreased attention during the session. Further investigations may be needed to relate the increase in ROM with an improvement in gesture smoothness.

Although the relatively low sample size limits the generalizability of the conclusions of this study and the absence of a control group does not allow us to show the potential of the device to exceed regular rehabilitation performance, the results in terms of accuracy of the measurements of the robot confirm that this device could serve to design future data-driven rehabilitation protocols, in alignment with the existing body of literature on personalized rehabilitation. Indeed, demonstrating that the robot can accurately measure clinically relevant variables is crucial for rehabilitation and could drive personalized treatments that could take into account the performance of the participants daily, making the treatment challenging at any time. The presented feasibility study lacks the evaluation of retention effects; while this evaluation was outside the scope of the study, future

studies will be more focused on evaluate the efficacy and will include follow-up measurements to assess the potential retention of the rehabilitation outcome, both in stereotyped flexion-extension movements and in functional movements or activities of daily. Given these points, the results of this pilot study encourage the conduction of a larger, longitudinal controlled study to further investigate the clinical efficacy of the device. Considering the overall experience in clinics, and after discussion with clinical personnel, the platform will be refined to be more intuitive in the wearing procedure and the system's calibration procedure, also including the possibility to selectively train more than one finger and ultimately to extend the architecture to multiple or full hand exoskeletons that can be used in functional tasks in the 3D space.

Conclusions

In this pilot study, a powered finger exoskeleton, namely I-Phlex, was used in a pilot clinical study to rehabilitate post-traumatic hands. Results show that the device and related rehabilitation exercises can be successfully used within the clinical rehabilitation of the MCP joint. Regarding efficacy, the results of this study show that a single-session treatment based on *passive* and *active-assistive* exercises can induce increases in the PROM and AROM when comparing pre- and post-treatment measurements. Joint angles and torques measured by the device are in line with the common methodology in terms of clinical assessment of ROM and demonstrated to complement the clinical measurements gathered by the therapist. Future studies will investigate the efficacy of the device with a larger pool of subjects and longer training sessions and consider a follow-up evaluation of the retention effects of the rehabilitation treatment. A control group will be included to compare the robotic treatment with conventional therapy.

Abbreviations

SCI	Spinal cord injury
MCP	Metacarpophalangeal
RCM	Remote center of motion
SEA	Series elastic actuation
R	Rotational (joint)
P	Prismatic (joint)
FPGA	Field programmable gate array
HLCL	High-level control layer
GUI	Graphical user interface
DKsM	Direct kineto-static model
LUT	Look-up table
MLCL	Middle-level control layer
IKsM	Inverse kineto-static model
LLCL	Low-level control layer
F/E cycle	Flexion/extension cycle
PROM	Passive range of motion
AROM	Active range of motion
IQR	Inter-quartile range
SPARC	Spectral arc length
RMSE	Root mean square error
NPRS	Numerical pain rate scale

Acknowledgements

We would like to thank all the participants who took part in the experiments.

Author contributions

S.L.C, T.F. and E.P. designed the prototype and implemented the control strategies. E.P., E.Tr., E.C, F. P., S. G., A. R., G. L, E.Ta, I.C., S.C. and N.V. designed the experimental protocol. I.C, E.Ta., F.P., S.G., A.R. and G.L. recruited the participants, performed the clinical evaluation of the patients and took part in the execution of the experimental protocol. E.P., E.C. and E.Tr performed the experiments. I.C., N.V., E.Ta and S.C. were the scientific supervisors of the study. E.P., E.C. and E. Tr. analysed the data and drafted the manuscript. All authors contributed to the discussion of the results and the thorough revision of the manuscript. All authors read and approved the final manuscript.

Funding

This work was supported by the Italian National Institute for Insurance Against Accidents at Work (Inail), in part by the HABILIS Project, and part by the HABILIS + + Project under Grant PR19-RR_P4.

Data availability

The datasets used and/or analyzed during the current study are available from the corresponding author upon reasonable request.

Declarations

Ethics approval and consent to participate

This study was approved by the Ethical Committee of Area Vasta Nord Ovest (Tuscany, Italy) and all participants provided written informed consent.

Consent for publication

Not applicable.

Competing interests

The authors declare no competing interests.

Author details

[1]The BioRobotics Institute, Scuola Superiore Sant'Anna, Pontedera, Pisa, Italy
[2]Department of Excellence in Robotics & AI, Scuola Superiore Sant'Anna, Pisa, Italy
[3]Inail Motor Rehabilitation Center (CRM), Volterra, Pisa, Italy

Received: 6 September 2023 / Accepted: 19 November 2024
Published online: 19 December 2024

References

1. Shi Q, Sinden K, MacDermid JC, Walton D, Grewal R. A systematic review of prognostic factors for return to work following work-related traumatic hand injury. J Hand Ther. 2014;27(1):55–62. https://doi.org/10.1016/j.jht.2013.10.001.
2. Poggetti A, Del Chiaro A, Nucci AM, Suardi C, Pfanner S. How hand and wrist trauma has changed during covid-19 emergency in Italy: incidence and distribution of acute injuries. What to learn? J Clin Orthop Trauma. 2021;12(1):22–6. https://doi.org/10.1016/j.jcot.2020.08.008.
3. Giustini M, Leo AD, Acciaro AL, Pajardi G, Mamo C, Voller F, Fadda F, Fondi G, Pitidis A. Incidence estimates of hand and upper extremity injuries in Italy. Ann Ist Super Sanita. 2015;51:305–12.
4. de Jong JP, Nguyen JT, Sonnema AJM, Nguyen EC, Amadio PC, Moran SL. The incidence of acute traumatic tendon injuries in the hand and wrist: a 10-year population-based study. Clin Orthop Surg. 2014;6(2):196. https://doi.org/10.4055/cios.2014.6.2.196.
5. Moellhoff N, Throner V, Frank K, Benne A, Coenen M, Giunta RE, Haas-Lützenberger EM. Epidemiology of hand injuries that presented to a tertiary care facility in Germany: a study including 435 patients. Arch Orthop Trauma Surg. 2023;143(3):1715–24. https://doi.org/10.1007/s00402-022-04617-9.
6. Kollitz KM, Hammert WC, Vedder NB, Huang JI. Metacarpal fractures: treatment and complications. Hand. 2014;9(1):16–23. https://doi.org/10.1007/s11552-013-9562-1.

7. Oo WM, Hunter DJ. Efficacy, safety, and accuracy of intra-articular therapies for hand osteoarthritis: current evidence. Drugs Aging. 2023;40(1):1–20. https://doi.org/10.1007/s40266-022-00994-3.
8. Gashaw M, Aragaw FM, Zemed A, Endalew M, Tsega NT, Asratie MH, Belay DG. Distal and/or proximal joint stiffness among post-fracture patients treated in University of Gondar Comprehensive Specialized Hospital, Gondar, Ethiopia. Orthop Res Rev. 2022;14:157–67. https://doi.org/10.2147/ORR.S365011.
9. Dogu B, Kuran B, Sirzai H, Sag S, Akkaya N, Sahin F. The relationship between hand function, depression, and the psychological impact of trauma in patients with traumatic hand injury. Int J Rehabil Res. 2014;37(2):105–9. https://doi.org/10.1097/MRR.0000000000000040.
10. Şahin F, Akca H, Akkaya N, Zincir ÖD, Işık A. Cost analysis and related factors in patients with traumatic hand injury. J Hand Surg Eur. 2013;38(6):673–9. https://doi.org/10.1177/1753193412469012.
11. Catalano LW, Barron OA, Glickel SZ, Minhas SV. Etiology, evaluation, and management options for the stiff digit. J Am Acad Orthop Surg. 2019;27(15):e676–84. https://doi.org/10.5435/JAAOS-D-18-00310.
12. Yang G, McGlinn EP, Chung KC. Management of the stiff finger. Clin Plast Surg. 2014;41(3):501–12. https://doi.org/10.1016/j.cps.2014.03.011.
13. Santacreu ES, Cabezas NV, Graupera AB. Combined treatment with paraffin, manual therapy, pegboard and splinting in a patient with post-traumatic stiff hand. Arch Physiother. 2016;6(1):14. https://doi.org/10.1186/s40945-016-0028-y.
14. Keller MM, Barnes R, Brandt C, Hepworth LM. Hand rehabilitation programmes for second to fifth metacarpal fractures: a systematic literature review. South Afr J Physiother. 2021;77(1). https://doi.org/10.4102/sajp.v77i1.1536.
15. Dent JA. Continuous passive motion in hand rehabilitation. Prosthet Orthot Int. 1993;17(2):130–5. https://doi.org/10.3109/03093649309164369.
16. Neumeister MW, Winters JN, Maduakolum E. Phalangeal and metacarpal fractures of the hand: preventing stiffness. Plast Reconstr Surg Glob Open. 2021;9(10):e3871. https://doi.org/10.1097/GOX.0000000000003871.
17. Li L, Tyson S, Weightman A. Professionals' views and experiences of using rehabilitation robotics with stroke survivors: a mixed methods survey. Front Med Technol. 2021;3:780090. https://doi.org/10.3389/fmedt.2021.780090.
18. Trigili E, Crea S, Moisè M, Baldoni A, Cempini M, Ercolini G, Marconi D, Posteraro F, Carrozza MC, Vitiello N. Design and experimental characterization of a shoulder-elbow exoskeleton with compliant joints for post-stroke rehabilitation. IEEE/ASME Trans Mechatron. 2019;24(4):1485–96. https://doi.org/10.1109/TMECH.2019.2907465.
19. Posteraro F, Crea S, Mazzoleni S, Berteanu M, Ciobanu I, Vitiello N, Cempini M, Gervasio S, Mrachacz-Kersting N. Technologically-advanced assessment of upper-limb spasticity: a pilot study. Eur J Phys Rehabil Med. 2018;54(4). https://doi.org/10.23736/S1973-9087.17.04815-8.
20. Pilla A, Trigili E, McKinney Z, Fanciullacci C, Malasoma C, Posteraro F, Crea S, Vitiello N. Robotic rehabilitation and multimodal instrumented assessment of post-stroke elbow motor functions—A randomized controlled trial protocol. Front Neurol. 2020;11:587293. https://doi.org/10.3389/fneur.2020.587293.
21. Sarac M, Solazzi M, Frisoli A. Design requirements of generic hand exoskeletons and survey of hand exoskeletons for rehabilitation, assistive, or haptic use. IEEE Trans Haptics. 2019;12(4):400–13. https://doi.org/10.1109/TOH.2019.2924881.
22. Noronha B, Accoto D. Exoskeletal devices for hand assistance and rehabilitation: a comprehensive analysis of state-of-the-art technologies. IEEE Trans Med Robot Bionics. 2021;3(2):525–38. https://doi.org/10.1109/TMRB.2021.3064412.
23. Tran P, Jeong S, Herrin KR, Desai JP. Review: hand exoskeleton systems, clinical rehabilitation practices, and future prospects. IEEE Trans Med Robot Bionics. 2021;3(3):606–22. https://doi.org/10.1109/TMRB.2021.3100625.
24. Noronha B, Ng CY, Little K, Xiloyannis M, Kuah CW, Wee SK, Kulkarni SR, Masia L, Chua KS, Accoto D. Soft, lightweight wearable robots to support the upper limb in activities of daily living: a feasibility study on chronic stroke patients. IEEE Trans Neural Syst Rehabil Eng. 2022;30:1401–11. https://doi.org/10.1109/TNSRE.2022.3175224.
25. Alicea R, Xiloyannis M, Chiaradia D, Barsotti M, Frisoli A, Masia L. A soft, synergy-based robotic glove for grasping assistance. Wearable Technol. 2021;2:e4. https://doi.org/10.1017/wtc.2021.3.
26. Tran P, Jeong S, Lyu F, Herrin K, Bhatia S, Elliott D, Kozin S, Desai JP. FLEXotendon glove-III: voice-controlled soft robotic hand exoskeleton with novel fabrication method and admittance grasping control. IEEE/ASME Trans Mechatron. 2022;27(5):3920–31. https://doi.org/10.1109/TMECH.2022.3148032.
27. Popov D, Gaponov I, Ryu J-H. Portable exoskeleton glove with soft structure for hand assistance in activities of daily living. IEEE/ASME Trans Mechatron. 2017;22(2):865–75. https://doi.org/10.1109/TMECH.2016.2641932.
28. Cappello L, Meyer JT, Galloway KC, Peisner JD, Granberry R, Wagner DA, Engelhardt S, Paganoni S, Walsh CJ. Assisting hand function after spinal cord injury with a fabric-based soft robotic glove. J Neuroeng Rehabil. 2018;15(1):59. https://doi.org/10.1186/s12984-018-0391-x.
29. Capotorti E, Trigili E, McKinney Z, Peperoni E, Dell'Agnello F, Fantozzi M, Baldoni A, Marconi D, Taglione E, Crea S, Vitiello N. A novel torque-controlled Hand Exoskeleton to Decode Hand Movements combining Semg and Fingers kinematics: a feasibility study. IEEE Robot Autom Lett. 2022;7(1):239–46. https://doi.org/10.1109/LRA.2021.3111412.
30. Cempini M, Cortese M, Vitiello N. A powered finger–thumb wearable hand exoskeleton with self-aligning joint axes. IEEE/ASME Trans Mechatron. 2015;20(2):705–16. https://doi.org/10.1109/TMECH.2014.2315528.
31. Esmatloo P, Deshpande AD. Fingertip position and force control for dexterous manipulation through model-based control of hand-exoskeleton-environment. In: 2020 IEEE/ASME international conference on advanced intelligent mechatronics (AIM). IEEE; 2020. pp. 994–1001. https://doi.org/10.1109/AIM43001.2020.9158879.
32. Li H, Cheng L, Li Z. Design and control of an index finger exoskeleton with cable-driven translational joints. In: 2020 5th international conference on advanced robotics and mechatronics (ICARM). IEEE; 2020. pp. 540–5. https://doi.org/10.1109/ICARM49381.2020.9195361.
33. Marconi D, Baldoni A, McKinney Z, Cempini M, Crea S, Vitiello N. A novel hand exoskeleton with series elastic actuation for modulated torque transfer. Mechatronics. 2019;61:69–82. https://doi.org/10.1016/j.mechatronics.2019.06.001.
34. Yurkewich A, Ortega S, Sanchez J, Wang RH, Burdet E. Integrating hand exoskeletons into goal-oriented clinic and home stroke and spinal cord injury rehabilitation. J Rehabil Assist Technol Eng. 2022;9:205566832211309. https://doi.org/10.1177/20556683221130970.
35. Bressi F, Santacaterina F, Cricenti L, Campagnola B, Nasto F, Assenza C, Morelli D, Cordella F, Lapresa M, Zollo L, Sterzi S. Robotic-assisted hand therapy with gloreha sinfonia for the improvement of hand function after pediatric stroke: a case report. Appl Sci. 2022;12(9):4206. https://doi.org/10.3390/app12094206.
36. Singh N, Saini M, Kumar N, Srivastava MVP, Mehndiratta A. Evidence of neuroplasticity with robotic hand exoskeleton for post-stroke rehabilitation: a randomized controlled trial. J Neuroeng Rehabil. 2021;18(1):76. https://doi.org/10.1186/s12984-021-00867-7.
37. Wilhelm NJ, Haddadin S, Lang JJ, Micheler C, Hinterwimmer F, Reiners A, Burgkart R, Glowalla C. Development of an exoskeleton platform of the finger for objective patient monitoring in rehabilitation. Sensors. 2022;22(13):4804. https://doi.org/10.3390/s22134804.
38. Peters SE, Jha B, Ross M. Rehabilitation following surgery for flexor tendon injuries of the hand. Cochrane Database Syst Rev. 2021;2021(1). https://doi.org/10.1002/14651858.CD012479.pub2.
39. Peperoni E, Capitani SL, Fiumalbi T, Capotorti E, Baldoni A, Dell'Agnello F, Creatini I, Taglione E, Vitiello N, Trigili E, Crea S. Self-aligning finger exoskeleton for the mobilization of the metacarpophalangeal joint. IEEE Trans Neural Syst Rehabil Eng. 2023;31:884–94. https://doi.org/10.1109/TNSRE.2023.3236070.
40. Vitiello N, Baldoni A, Crea S, Scalamogna A, Fiumalbi T. Kinematic chain to assist flexion-extension of a joint. Volume 30. IT102019000017558; 2019.
41. Tucker MR, Olivier J, Pagel A, Bleuler H, Bouri M, Lambercy O, Millán JD, Riener R, Vallery H, Gassert R. Control strategies for active lower extremity prosthetics and orthotics: a review. J Neuroeng Rehabil. 2015;12(1). https://doi.org/10.1186/1743-0003-12-1.
42. Balasubramanian S, Melendez-Calderon A, Roby-Brami A, Burdet E. On the analysis of movement smoothness. J Neuroeng Rehabil. 2015;12(1):112. https://doi.org/10.1186/s12984-015-0090-9.
43. Gomez-Donoso F, Escalona F, Nasri N, Cazorla M. A hand motor skills rehabilitation for the injured implemented on a social robot. Appl Sci. 2021;11(7):2943. https://doi.org/10.3390/app11072943.
44. Baldan F, Turolla A, Rimini D, Pregnolato G, Maistrello L, Agostini M, Jakob I. Robot-assisted rehabilitation of hand function after stroke: development of prediction models for reference to therapy. J Electromyogr Kinesiol. 2021;57:102534. https://doi.org/10.1016/j.jelekin.2021.102534.
45. Scotto di Luzio F, Cordella F, Bravi M, Santacaterina F, Bressi F, Sterzi S, Zollo L. Modification of hand muscular synergies in stroke patients after robot-aided rehabilitation. Appl Sci. 2022;12(6):3146. https://doi.org/10.3390/app12063146.

46. Gobbo M, Gaffurini P, Vacchi L, Lazzarini S, Villafane J, Orizio C, Negrini S, Bissolotti L. Hand passive mobilization performed with robotic assistance: acute effects on upper limb perfusion and spasticity in stroke survivors. Biomed Res Int. 2017;2017:1–6. https://doi.org/10.1155/2017/2796815.
47. Serrano-López PA, Terradas T, Criado Ferrer I, Jakob, Calvo-Arenillas JI. Quo vadis, amadeo hand robot? A randomized study with a hand recovery predictive model in subacute stroke. IJERPH. 2022;20(1):690. https://doi.org/10.3390/ijerph20010690.
48. Jo I, Park Y, Lee J, Bae J. A portable and spring-guided hand exoskeleton for exercising flexion/extension of the fingers. Mech Mach Theory. 2019;135:176–91. https://doi.org/10.1016/j.mechmachtheory.2019.02.004.
49. Tamantini C, Cordella F, Lauretti C, di Luzio FS, Bravi M, Bressi F, Draicchio F, Sterzi S, Zollo L. Patient-tailored adaptive control for robot-aided orthopaedic rehabilitation. In: 2022 international conference on robotics and automation (ICRA). IEEE; 2022. pp. 5434–40. https://doi.org/10.1109/ICRA46639.2022.9811791.
50. Reissner L, Fischer G, List R, Taylor WR, Giovanoli P, Calcagni M. Minimal detectable difference of the finger and wrist range of motion: comparison of goniometry and 3D motion analysis. J Orthop Surg Res. 2019;14(1):173. https://doi.org/10.1186/s13018-019-1177-y.
51. 'About HAKIR. – HAKIR – Handkirurgiskt kvalitetsregister'. Accessed: Jun. 27, 2023. [Online]. Available: https://hakir.se/about-hakir/
52. Escott BG, Ronald K, Judd MGP, Bogoch ER. NeuFlex and Swanson Metacarpophalangeal Implants for Rheumatoid Arthritis: prospective randomized, controlled clinical trial. J Hand Surg. 2010;35(1):44–51. https://doi.org/10.1016/j.jhsa.2009.09.020.
53. Casas R, Sandison M, Nichols D, Martin K, Phan K, Chen T, Lum PS. Home-based therapy after stroke using the hand spring operated movement enhancer (HandSOME II). Front Neurorobot. 2021;15:773477. https://doi.org/10.3389/fnbot.2021.773477.
54. Haarman CJW, Hekman EEG, Rietman JS, Van Der Kooij H. Mechanical design and feasibility of a finger exoskeleton to support finger extension of severely affected stroke patients. IEEE Trans Neural Syst Rehabil Eng. 2023;31:1268–76. https://doi.org/10.1109/TNSRE.2023.3243357.
55. Samhan AF, Abdelhalim NM, Elnaggar RK. Effects of interactive robot-enhanced hand rehabilitation in treatment of paediatric hand-burns: a randomized, controlled trial with 3-months follow-up. Burns. 2020;46(6):1347–55. https://doi.org/10.1016/j.burns.2020.01.015.
56. Brooke J. SUS-A quick and dirty usability scale. In: Usability evaluation in industry. vol. 189. 1996. pp. 4–7.
57. Di Guardo A, Sarac M, Gabardi M, Leonardis D, Solazzi M, Frisoli A. Sensitivity analysis and identification of human parameters for an adaptive, underactuated hand exoskeleton. In: Lenarcic J, Parenti-Castelli V, editors. Advances in robot kinematics. Springer proceedings in advanced robotics, vol. 8. Cham: Springer International Publishing; 2019. pp. 449–57. https://doi.org/10.1007/978-3-319-93188-3_51.
58. Casas R, Martin K, Sandison M, Lum PS. A tracking device for a wearable high-DOF passive hand exoskeleton. In: 2021 43rd annual international conference of the IEEE engineering in medicine & biology society (EMBC). IEEE; 2021. pp. 6643–6. https://doi.org/10.1109/EMBC46164.2021.9630403.
59. Unsworth A, Bey PMA, Haslock I. Stiffness in the metacarpo-phalangeal joints of young adults. Clin Phys Physiol Meas. 1981;2(2):123–33. https://doi.org/10.1088/0143-0815/2/2/001.

Publisher's note